Dipolar NMR Strategies for Multispin Systems Involving Quadrupolar Nuclei: $^{31}P\{^{23}Na\}$ Rotational Echo Double Resonance (REDOR) of Crystalline Sodium Phosphates and Phosphate Glasses

Wenzel Strojek, Martin Kalwei, and Hellmut Eckert*

Institut für Physikalische Chemie, Westfälische Wilhelms−Universität Münster, Corrensstrasse 30, D-48149 Münster, Germany

Received: October 9, 2003; In Final Form: March 17, 2004

A new procedure for the site-selective measurement of heteronuclear magnetic dipole−dipole interactions involving quadrupolar nuclei has been developed. Particular attention is given to the case of $S\{I\}$ rotational echo double resonance (REDOR) with $S = {}^1/_2$ and $I = {}^3/_2$, where the nuclear electric quadrupole splitting affects the efficiency of the $\pi(I)$ pulses in recoupling the $S-I$ dipolar interactions. Detailed two- and three-spin simulations using the SIMPSON code indicate that the REDOR response is sensitively affected by the quotient of the nutation frequency and the nuclear electric quadrupole frequency (ν_1/ν_q). Multispin systems can be conveniently analyzed using a curvature determination of REDOR data in the limit of short dipolar evolution times ($\Delta S/S_0 < 0.2$), to yield dipolar second moment (M_2) values. The apparent M_2 values measured in this fashion include a scaling factor f_1, the magnitude of which can be predicted if ν_1/ν_q is known. Based on this finding, a robust method has been developed to analyze experimental REDOR data in multispin systems, in terms of average dipolar M_2 values, which are shown to be affected by distributions of magnetic dipolar and nuclear electric quadrupolar coupling constants only to a minor extent. Validation experiments on suitable model compounds indicate that dipolar M_2 values can be measured within 10% accuracy in this fashion for crystalline compounds. For glasses, the error may be higher, because of possible cumulative errors that may occur from unknown geometries and distribution effects. Experiments conducted on glassy sodium phosphates indicate that the $^{31}P-^{23}Na$ dipolar interaction strengths in these systems are differentiable for the various $Q^{(n)}$ sites and increase as the charge of the phosphate moiety increases.

Introduction

Magic-angle spinning (MAS) NMR spectroscopy has become an immensely useful experimental probe method for the structural analysis of disordered materials.[1] Several sophisticated techniques have been developed to tailor, separate, and quantify the various internal interaction parameters carrying structural information.[2,3] Among the latter, the magnetic dipole−dipole coupling constants possess special significance, because of their simple relationship with internuclear distances and distance distributions. MAS, by its very design, averages out such interactions; therefore, the implementation of appropriate recoupling strategies has remained an important objective of NMR technique development. In this regard, the rotational echo double resonance (REDOR) method has proven very useful for the accurate measurement of internuclear distances between unlike nuclei.[4,5] In its original design, REDOR reintroduces the heteronuclear dipolar interaction between two nuclear species S and I into the MAS experiment, by the application of π-pulse trains to the I-spins during the rotor cycle. The signal intensity observed for the S-nuclei is diminished if a dipolar interaction is present, and the latter can be quantified by plotting the normalized difference signal ($\Delta S/S_0$) versus the dipolar evolution time. Using this approach, internuclear distances up to 10 Å have been determined within isolated pairs of spin $-{}^1/_2$ nuclei in a great variety of biological solids.[5−7]

Several successful applications of REDOR to inorganic solids and glasses have also been published,[8−18] although many complications can intervene. First of all, the three-dimensional connectivities present in such inorganic networks, combined with the high natural abundances of the nuclear isotopes present, have a tendency to produce multiple-spin interactions, affecting the REDOR curves in a way that is strongly dependent on the details of the local molecular architecture.[19,20] Although highly specific geometry information might be obtained if the systems under study present isolated clusters of a few spins only, such an ideal situation rarely exists in inorganic solids. Second, in the case of disordered systems and glasses, one usually does not even know the order and the geometry of the spin system, and the distance geometry may well be rather ill-defined, because of a spread of internuclear distances and bond angles. As we have previously shown, both of the aforementioned problems can be circumvented by confining the REDOR data analysis to the initial curvature, where $\Delta S/S_0 < 0.2$.[20−22] In this limit of short dipolar evolution times, the REDOR curve is found to be geometry-independent and dominated by the van Vleck second moment (M_2), which can serve as a useful quantitative criterion for testing hypothetical atomic distribution models.[23] Previous simulations have also shown that the effects of homonuclear $I-I$ interactions and experimental imperfections can be minimized in this time regime.[21,24] A third important

* Author to whom correspondence should be addressed. E-mail address: eckerth@uni-muenster.de.

10.1021/jp037041c CCC: $27.50
Published on Web 05/05/2004

complication arises from the fact that many of those nuclei found in inorganic network glasses possess $I > {}^1/_2$, i.e., they are generally affected by nuclear electric quadrupolar interactions. The ensuing resonance splitting causes a significant reduction in the $\Delta S\{I\}/S_0$ difference signal, because the efficiency of the $\pi(I)$-pulse trains to manipulate the corresponding *I*-spin Zeeman populations is seriously compromised and even difficult to predict theoretically. To overcome this problem, alternative techniques such as the transfer of populations with double resonance (TRAPDOR) method[25,26] and the rotational echo adiabatic passage double resonance (REAPDOR) method[27−29] have been designed. In both of these techniques, the *I*-spin flips needed for $I-S$ dipolar recoupling are caused by adiabatic passages between the quadrupolar-perturbed Zeeman states of the *I* nuclei. They always occur when the quadrupolar splitting, which becomes time-dependent, because of MAS, crosses through zero during the pulse. Although both TRAPDOR and REAPDOR use simpler methods (continuous irradiation or application of single pulses) for *I*-spin state manipulation, the spin dynamics involved are still fairly complex. A valid data analysis then requires very detailed information about the interaction tensor components and, in the case of TRAPDOR, mutual tensor orientations as well.[30] Such information is usually not available in disordered materials. Finally, quantitative treatments of TRAPDOR and REAPDOR have thus far been limited to the two-spin case, and generalizations to multiple-spin interactions remain to be done.

In the present contribution, the aforementioned issues will be addressed in detail, using both theoretical simulations and experimental studies on model compounds with well-defined distance geometries. Specifically, we will develop a generally applicable procedure to extract reliable dipole−dipole coupling information from REDOR and/or REAPDOR curves of multi-spin systems that involve quadrupolar nuclei. Our method will be tested against experimental $^{31}P\{^{23}Na\}$ REDOR data on crystalline sodium phosphates and subsequently applied to the structural analysis of sodium phosphate glasses.

Theoretical Background and Methodology

REDOR theory involving isolated $S-I$ spin pairs (S, $I = {}^1/_2$) is now well-established.[3] The experiment measures the magnitude of a difference signal obtained in the absence (magnitude S_0) and the presence (reduced magnitude S) of a heteronuclear dipole−dipole interaction in the MAS Hamiltonian. To achieve the latter, a variety of pulse sequences are available.[3] A sequence well-suited to the experimental analysis of multispin systems in particular is shown in Figure 1.[31] Following preparation by a $\pi/2$ pulse, the transverse observed (S) spin magnetization is flipped back and forth by a series of π-pulses applied both in the middle of the rotor period and on completion of a rotor cycle. This manipulation inverts the sign of the heteronuclear dipolar coupling constant during each individual rotor period, thereby interfering with the ability of MAS to remove the interaction from the spin Hamiltonian. It can be shown, however, that the omission of a single $\pi(S)$-pulse after n rotor cycles results in a complete cancellation of the heteronuclear dipolar interaction after $2n$ rotor cycles, producing the reference signal S_0. It is then possible to reintroduce the $I-S$ interaction by flipping the *I*-spins in the middle of the dipolar evolution period (i.e., after n rotor cycles), resulting in a reduced signal of amplitude S at the point of acquisition (after $2n$ rotor cycles). The normalized difference signal $\Delta S/S_0$ can be

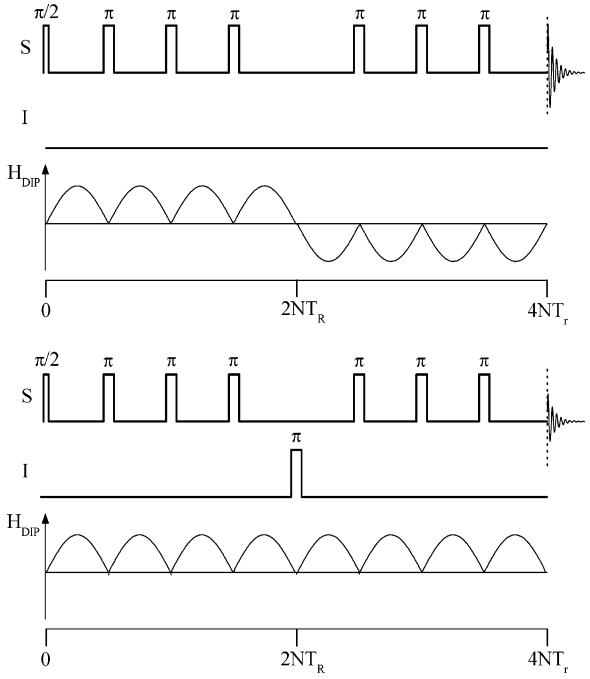

Figure 1. Timing diagram of the rotational echo double resonance (REDOR) pulse sequence used in the present study. The top portion of the figure shows the obtention of the reference signal S_0, and the bottom portion shows the reintroduction of the dipolar interaction by the $\pi(I)$-pulse. The evolution of the heteronuclear dipolar Hamiltonian (tensor orientation $\alpha = 0°$, $\beta = 180°$) at each stage also is sketched.

calculated using Average Hamiltonian Theory. For a powdered sample,[3]

$$\frac{\Delta S}{S_0} = 1 - \frac{1}{4\pi}\int_0^{2\pi} d\alpha \int_0^{\pi} \sin\beta \cos(\Delta\Phi)\, d\beta \qquad (1)$$

In this expression, $\Delta\Phi$ is the dipolar dephasing angle given by the product of the dipolar coupling constant D and the dipolar evolution time (NT_r, defined as the number of rotor cycles ($2n$) multiplied by the rotor period):

$$\Delta\Phi = 4\sqrt{2}NT_rD \sin\beta \cos\beta \sin a \qquad (2)$$

For two-spin systems, a useful analytical solution has been given by Mueller:[32]

$$\frac{\Delta S}{S_0} = 1 - [J_0(\sqrt{2}\lambda_N)]^2 + 2\sum_{k=1}^{\infty}\frac{1}{16k^2-1}[J_k(\sqrt{2}\lambda_N)]^2 \qquad (3)$$

where J_k are kth-order Bessel functions of the first type.

The aforementioned expression is still valid if the observed nuclei (S) possess a spin quantum number $> {}^1/_2$ and are subject to first- or second-order nuclear electric quadrupolar perturbations. This is due to the fact that the quadrupolar interaction affects both the intensities S and S_0 equally, so that the overall effect is canceled out in the difference experiment. In contrast, the situation is different for the dephasing of spin echoes in the dipolar field of $I > {}^1/_2$ nuclei. In this case, one must take into account that the different possible Zeeman states m_I for these nuclei differ in their respective magnitude of their z-components and, hence, generate dipolar fields of different magnitudes at the observed spins.[33,34] Therefore, expression 3 must be replaced by a weighted superposition of $2I + 1$ individual dephasing curves. At sufficiently high temperatures ($T > 1$ K), the populations of all of these states are ap-

proximately equal, and, thus, we obtain

$$\frac{\Delta S}{S_0} = \frac{1}{2I+1}\sum_{m=-I}^{I}\left(1 - [J_0(2\sqrt{2}|m|\lambda_N)]^2 + 2\sum_{k=1}^{\infty}\frac{1}{16k^2-1}[J_k(2\sqrt{2}|m|\lambda_N)]^2\right) \quad (4)$$

In the case of $I = {}^3/_2$, which is of particular interest in the present study, eq 4 becomes

$$\frac{\Delta S}{S_0} = 0.5\left\{1 - [J_0(\sqrt{2}\lambda_N)]^2 + 2\sum_{k=1}^{\infty}\frac{1}{16k^2-1}[J_k(\sqrt{2}\lambda_N)]^2\right\} + 0.5\left\{1 - [J_0(3\sqrt{2}\lambda_N)]^2 + 2\sum_{k=1}^{\infty}\frac{1}{16k^2-1}[J_k(3\sqrt{2}\lambda_N)]^2\right\} \quad (5)$$

taking into account the fact that the dipolar field produced by the $|m_I| = {}^3/_2$ states is three times as large as that resulting from the $|m_I| = {}^1/_2$ states. However, this expression remains valid only in the limit of zero or very weak nuclear electric quadrupolar interactions (coupling constants of $C_q < 50$ kHz). For larger C_q values, the anisotropic broadening of the $|{}^1/_2\rangle \leftrightarrow |{}^3/_2\rangle$ "satellite transitions" produces large resonance offsets, which reduce the efficiency of the π-pulses to cause population inversion. The decisive parameter in this regard is the ratio ν_1/ν_q, where ν_1 is the nutation frequency of the I spins, which is governed by the amplitude of the radio-frequency (rf) pulses, and $\upsilon_q = 3C_q/[2I(2I-1)]$ is the quadrupolar frequency. For sufficiently strong quadrupolar interactions, as ν_1/ν_q approaches zero, only the central $|{}^1/_2\rangle \leftrightarrow |{}^{-1}/_2\rangle$ coherences will be affected. In this limiting case, only those S-spins that are coupled to nuclei in Zeeman states with $|m_I| = {}^1/_2$ yield a REDOR response, at least under the ideal conditions that the π-pulses applied to the I-spins are infinitely short.

The present study involves situations of inevitable experimental realities and complications that preclude us to analyze REDOR data sets via eq 5, because there are (i) nuclear electric quadrupolar coupling of intermediate strengths; (ii) finite-pulse-length effects, leading to adiabatic mixing between different m_I states during the rotor cycle; and (iii) multispin dipolar interactions. These complications must be addressed by calculating numerically the stepwise propagation of the density matrix under the time-dependent Hamiltonian, taking into account explicitly the experimental parameters used. This approach has recently become possible using the publicly available SIMPSON program package.[35] Here, we wish to present simulations for the $S\{I = {}^3/_2\}$ REDOR case, which is particularly relevant for dipolar coupling studies of many inorganic materials. In doing so, we will also extend the analysis to include distributions of dipolar and nuclear electric quadrupolar coupling constants, all of which are important features of the disordered inorganic state of matter.

Effect of Nuclear Electric Quadrupole Interactions on $S\{I = {}^3/_2\}$ REDOR Curves. Figure 2 shows ^{31}P{^{23}Na} REDOR curves ($\Delta S/S_0$ vs NT_rD), simulated for the pulse sequence of Figure 1, as applied to a two-spin system. The following parameters were used: spinning speed, 15 kHz; and 180° pulse length, 5.0 μs for ^{31}P, respectively. These terms reflect a typical set of experimental conditions applicable to the structural analysis of glasses at high resolution with commercially available equipment. The π-pulse length of ^{23}Na corresponds to a nutation frequency of $\nu_1 = 55$ kHz in a liquid sample. The magnitude of the ^{23}Na nuclear electric quadrupolar coupling constant C_q has been systematically varied in these simulations, and an arbitrary value of the electric field gradient (EFG) asymmetry parameter η has been assumed ($\eta = 0.5$). The orientation of the EFG principal axis, with respect to the ^{31}P−^{23}Na dipolar vector was varied systematically; however, the effect on the calculated REDOR curves is found to be minimal, in agreement with the previously reported REAPDOR simulations.[29,30] Consequently, most of the subsequent simulations were performed by assuming coincident dipole and EFG tensors.

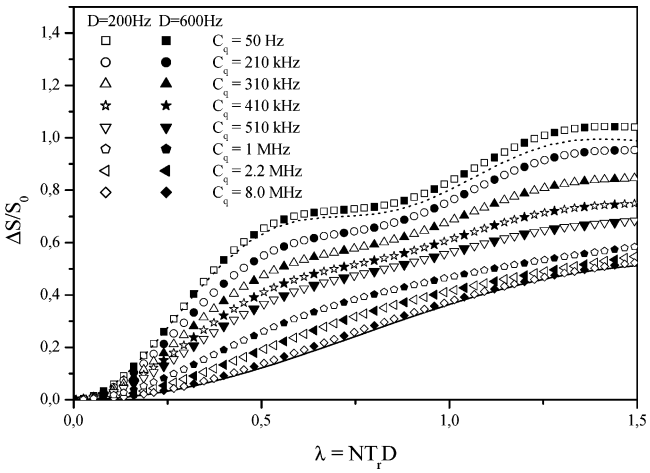

Figure 2. Effect of the nuclear electric quadrupolar coupling constant (C_q) on the universal $S\{I\}$ REDOR curves of a two-spin system. Simulations assume $I = {}^3/_2$, $S = {}^1/_2$, $\nu_1^{(I)} = 55$ kHz, $\nu_r = 15$ kHz, and an arbitrarily chosen asymmetry parameter ($\eta = 0.5$) of the electric field gradient (EFG) tensor. For each value of C_q, the correct $\pi(I)$-pulse length was determined by SIMPSON simulation and used in the calculation of the REDOR curve. Open and closed symbols represent results calculated for different magnitudes of the dipolar coupling constant, proving that the curves are indeed universal. Dotted line represents the theoretical behavior predicted by eq 5, whereas the solid line represents the theoretical behavior predicted by eq 5 in the limit of entirely selective excitation of the central coherence.

Figure 2 shows that, for small C_q values, the two-component behavior as predicted by eq 5 is readily apparent. With increasing magnitude of the C_q value, however, the REDOR response is successively attenuated, reflecting the fact that the spins in the outer $|\pm{}^3/_2\rangle$ Zeeman states are less and less affected by the $\pi(I)$-pulses. Note that the simulated curves approach the limiting cases (calculated via eq 5) of entirely nonselective irradiation of all the Zeeman states (the upper dotted curve in Figure 2) and entirely selective irradiation of the $|{}^1/_2\rangle \leftrightarrow |{}^{-1}/_2\rangle$ coherence (the lower solid curve in Figure 2) of the I-nuclei. (The small deviations that are observed will be discussed later.) Most importantly, for any value of C_q considered, the REDOR curves do not seem to be dependent on the D values used in the simulations, ($D = 200$ Hz (open symbols in Figure 2) and $D = 600$ Hz (filled symbols, in Figure 2)), indicating that they represent universal curves.

REDOR Curvature Analysis. Extending our previous approach, which was developed for spin $-{}^1/_2$ systems, to the case of higher-spin nuclei, the early portion of the universal REDOR curve (eq 4) can be approximated by a sum of parabolic functions:

$$\frac{\Delta S}{S_0} = \frac{1}{2I+1}\left[\sum_{m=-I}^{I}(2m)^2\right]\frac{1}{\pi^2(I+1)I}(NT_r)^2M_2 \quad (6)$$

Such an approximation permits determination of a dipolar second moment M_2 from an analysis of the curvature. This approximation is valid for $\Delta S/S_0 < 0.2$. Equation 6 holds only

for a nuclear electric quadrupolar coupling constant near zero. For the sake of quantitative analysis, we now introduce a phenomenological efficiency factor f_1 ($0 < f_1 < 1$) that takes into account the extent to which the dipolar coupling of *S*-spins to *I* nuclei in their outer Zeeman states influences the REDOR curve. Therefore, we make the substitution

$$\sum_{m=-3/2}^{+3/2} (2m)^2 \rightarrow (2(-^1/_2))^2 + (2(+^1/_2))^2 + (2(-^3/_2))^2 f_1 + (2(+^3/_2))^2 f_1 = 2 + 18f_1 \quad (7)$$

resulting in

$$\frac{\Delta S}{S_0} = \frac{1}{15\pi^2}(2 + 18f_1)(NT_r)^2 M_2 \quad (8)$$

By fitting the two-spin REDOR simulations of Figure 2 at short dipolar evolution times to parabolic curves according to eq 8, we can thus determine the value of f_1 for each specific magnitude of C_q (see Figure 3a) if the rf field strength characterized by the nutation frequency ν_1 is known. As illustrated in Figure 3b, f_1 increases as the ν_1/ν_q ratio increases, because the increased excitation bandwidth produces an increased contribution of the outer *I* Zeeman states to *S*-spin dephasing. In the other limit ($\nu_1/\nu_q \rightarrow 0$), f_1 becomes increasingly insensitive to this effect and approaches the limiting value of zero, as expected. Simulations performed at two fixed C_q values of 0.7 and 2.2 MHz indicate further that the value of the EFG asymmetry parameter η influences the REDOR curves, resulting in slightly different f_1 values from parabolic fitting. As revealed in Figure 3c, the dependence is non-monotonic, however, and significant changes are observed only at fairly large η values ($\eta > 0.6$).

Effect of Finite Pulse Lengths. As revealed by Figure 2, for the limits of very small and very large ν_1/ν_q ratios, the numerically calculated curves deviate slightly from those calculated via eq 5. These discrepancies arise from the fact that eq 5 is applicable only if the pulse sequence of Figure 1 applies perfect, infinitely short π-pulses to the *I*-spins. Whenever pulses of finite length are applied during the MAS rotation, they can induce adiabatic mixing of the m_I Zeeman states, causing additional *S*-spin dephasing (because of an implicit REAPDOR effect). The extent of this mixing is dependent on the adiabaticity parameter $\alpha = \nu_1^2/(\nu_r\nu_q)$ and, thus, is expected to decrease as the spinning speed increases. On the other hand, for finite pulse lengths, an increased spinning speed implies an increased duty cycle (the fraction of the rotor cycle occupied by rf irradiation) and, hence, should result in an increased probability of level crossings. The maximum REAPDOR effect has been previously shown to correspond to a duty cycle of ~33%.[36] Although in the present study, the duty cycles used generally are significantly smaller, an implicit REAPDOR effect in our REDOR studies warrants special consideration, as detailed below.

The aforementioned observations indicate the dephasing of *S*-spins in the dipolar field of quadrupolar nuclei is influenced by a complex interplay of *I*-spin nutation behavior, contributions of outer *I* Zeeman states to *S*-spin dephasing, and adiabatic mixing at finite duty cycles. Figure 4 shows the influence of C_q on the extent of $S\{I\}$ dephasing by plotting $\Delta S/S_0$ versus pulse length for a fixed dipolar evolution time (1.9 ms). For $C_q \approx 0$, $\Delta S/S_0$ shows the oscillatory behavior expected for the regular REDOR case. As C_q increases, the REDOR curve is attenuated, because of the reduced extent to which the $|m_I| = {}^3/_2$ Zeeman states contribute to *S*-spin dephasing. Furthermore, the complex nutation characteristics in the intermediate regime where $\nu_1/\nu_q \approx 1$ lead to a disappearance of the oscillatory

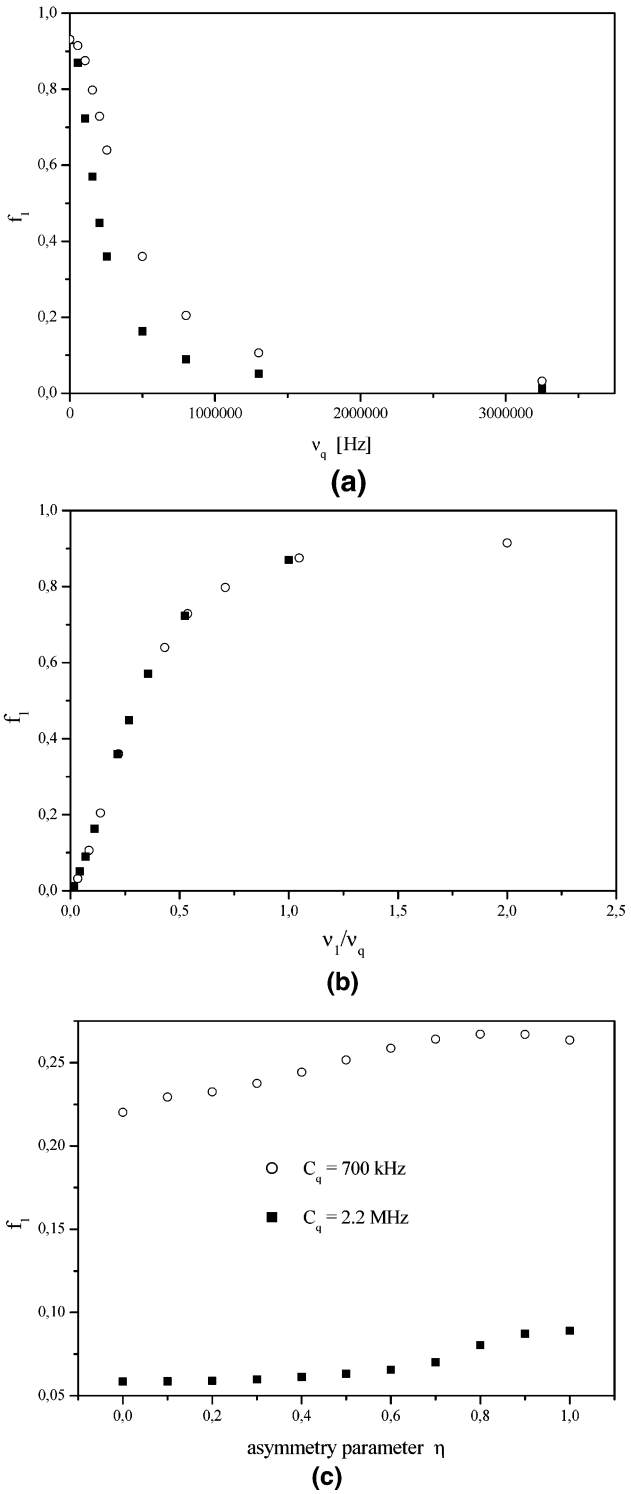

Figure 3. Influence of the nuclear electric quadrupolar coupling frequency ν_q (Hz) ($\eta = 0.5$) on the fitting parameter f_1, according to eq 8 ((a) simulation result for (■) $\nu_1 = 55$ kHz and (○) $\nu_1 = 110$ kHz, and (b) plot of f_1, as a function of ν_1/ν_q ((○) ^{23}Na nutation frequency = 110 kHz and (■) ^{23}Na nutation frequency = 55 kHz; small values of ν_1/ν_q correspond to a selective excitation of the quadrupolar nucleus, and larger values to a nonselective excitation). Panel c shows the influence of the EFG asymmetry parameter η on the curvature parameter f_1 for two fixed values of C_q (0.7 and 2.2 MHz, respectively). Simulations assume $\nu_1 = 55$ kHz and $\nu_r = 15$ kHz.

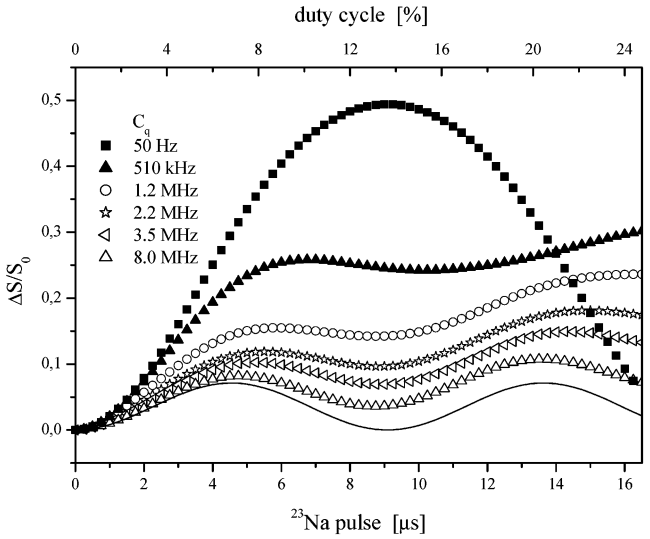

Figure 4. Magnitude of $\Delta S/S_0$ of the REDOR difference signal versus the pulse length for $D = 200$ Hz and a fixed dipolar evolution time (1.9 ms) and varying C_q values ($\eta = 0.5$). The solid curve approximated by $(1 - \cos \theta)/2$ shows the theoretically expected behavior in the absence of adiabatic spin-state transfers. Note that this latter effect increases as the ^{23}Na pulse length (duty cycle) increases.

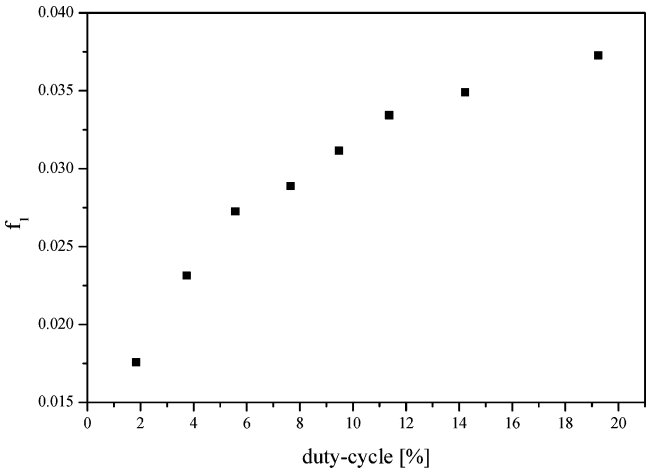

Figure 5. Plot of the factor f_1 versus the duty cycle, showing an increased contribution of adiabatic passages in the total dephasing with increasing duty cycle. Simulation parameters are $C_q = 2.2$ MHz and $\eta = 0.5$. A ^{23}Na nutation frequency of $\nu_1 = 30$ kHz was assumed. The duty cycle was systematically changed by varying MAS spinning frequencies over the range of 2−20 kHz.

behavior, and pulse length optimization on the basis of $\Delta S/S_0$ becomes impossible. As C_q is increased further, the oscillatory behavior reappears and the $\Delta S/S_0$ maximum shifts to a pulse length value that is half that observed for $C_q = 0$, signifying the approach toward the selective *I*-spin nutation limit. Still, inspection of Figure 4 reveals extra dephasing beyond that expected for a pure REDOR effect (solid curve), even in the selective excitation limit. We attribute these deviations to the implicit REAPDOR effect mentioned previously. The extent of this extra dephasing has a tendency to increase as the duty cycle increases, because the rf irradiation occupies a larger fraction of the MAS rotor period.[36] This was verified by explicit SIMPSON simulations performed for a fixed ν_1/ν_q ratio at different duty cycles, which were varied in the calculations by altering the MAS rotation speed. Figure 5 shows that the fitting parameter f_1 (obtained by parabolic fitting) increases as the duty cycle increases, reflecting the increased contribution of adiabatic passages to the REDOR difference signal. Principally, this same type of behavior is observed in the cases of small, intermediate, and large C_q values (0.7, 2.2, and 8.0 MHz, respectively; data not shown).

The need to optimize the resolution and minimize the spinning sideband effects usually requires the use of moderately high MAS spinning speeds. Thus, in our further considerations, we do not treat the MAS spinning rate as a freely variable parameter, but rather assume a constant spinning frequency of 15 kHz, which corresponds to the current state of the art with widely available commercial equipment.

Experimental Section

The crystalline sodium phosphate model compounds were purchased from Aldrich and used as received. Their purity was ascertained on the basis of powder X-ray diffraction (XRD) and ^{31}P MAS NMR spectroscopy. The two sodium phosphate glasses were prepared using standard melt-quenching procedures. Glass containing 35 mol % Na_2O was prepared by melting a mixture of $NaPO_3$ and P_2O_5 in the calculated proportions at 800 °C within an evacuated silica ampule. The melt was subsequently air-quenched by removing the sample from the furnace. Glass containing 60 mol % Na_2O was prepared by melting calculated proportions of NaH_2PO_4 and Na_2CO_3 in the open atmosphere at 800 °C within a platinum container, followed by air quenching (removal from the furnace). All the NMR experiments were performed on a Bruker model DSX 500 spectrometer that was equipped with a 4-mm high-speed spinning probe operating at 15 kHz. Single-pulse spectra were obtained at the resonance frequencies of 132.2 MHz (^{23}Na) and 202.4 MHz (^{31}P), using the following conditions: 90° pulse lengths of 5 and 6 μs (for ^{23}Na and ^{31}P, respectively) and relaxation delays of 10 and 60 s (for ^{23}Na and ^{31}P, respectively). In addition, the ^{23}Na nuclear electric quadrupolar interactions were characterized by 3Q-MAS, using the three-pulse sequence with zero quantum filtering. The ^{31}P{^{23}Na} REDOR studies were conducted using specifically designed probe circuitry, enabling experiments involving arbitrary combinations of X nuclei and ^{31}P spins. The following typical experimental parameters were used for these studies: 90° pulse lengths of 5 and 6 μs (for ^{23}Na and ^{31}P, respectively); a relaxation delay of 90 s; and spinning speeds of 10−15 kHz. The π-pulses on the *S*-channel were phase-cycled according to the XY8 scheme.[5] For each value of dipolar evolution time, the two parts of the REDOR sequence, leading to the amplitudes S_0 and S, were executed "back-to-back", thereby minimizing the effects of long-term instrumental drifts. To ensure reproducible initial conditions, the pulse sequence was preceded by a saturation comb for each data point. All the computations were done with SIMPSON (version 1.1.0) on LINUX computers (at 0.6−2.4 GHz) in the cluster mode.

Results and Data Analysis

Analysis Procedure for Experimental REDOR Data. The aforementioned considerations lead to the scheme shown in Figure 6, which summarizes a widely applicable REDOR−NMR strategy for the dipolar analysis of disordered multispin systems involving quadrupolar nuclei. Based on a nuclear electric quadrupolar coupling constant C_q (known from experiment), a universal REDOR curve is computed via SIMPSON, at the precise experimental conditions used for the REDOR experiment that has been performed. This simulation curve is fitted to a parabola, resulting in the appropriate f_1 value, which is then applicable for the analysis of the experimental data set. Using the f_1 value determined in this fashion, the experimental data set is fitted to eq 8, resulting in an experimental M_2 value. This

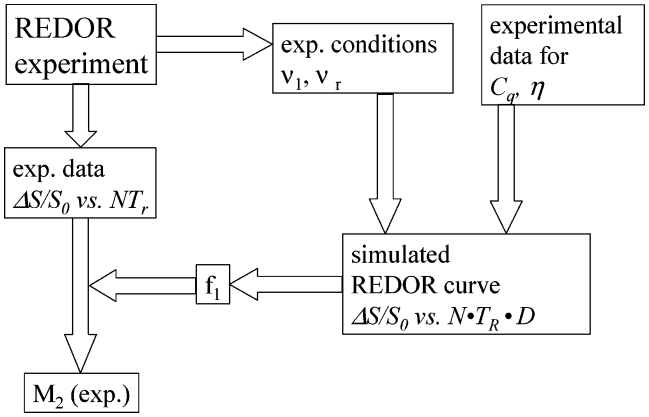

Figure 6. Schematic showing the proposed strategy for measuring heteronuclear dipole couplings between spin $-1/2$ and half-integer quadrupolar nuclei.

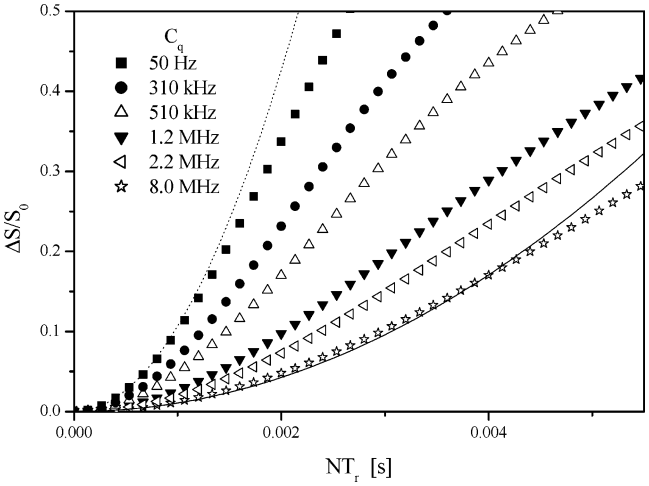

Figure 7. REDOR simulations for a three-spin system (^{23}Na$-^{31}$P$-^{23}$Na) for different C_q values ($\eta = 0.5$). The Na$-$P internuclear distances were chosen to be 0.5 nm. The angle between the internuclear vectors is $\zeta = 30°$. The SIMPSON simulations were performed assuming $\nu_1 = 55$ kHz and $\nu_r = 15$ kHz. In addition, the nonselective case with $f_1 = 1$ (dotted line) and the selective case with $f_1 = 0$ (solid line) are sketched. The first situation ($f_1 = 1$) is identical to a parabolic fit of the nonselective case ($C_q = 50$ Hz) in the data range $\Delta S/S_0 < 0.2$, whereas the second situation ($f_1 = 0$) is identical to a fit of the selective case ($C_q = 8.0$ MHz) up to $\Delta S/S_0 < 0.2$.

value can then be compared with a M_2 calculation from the van Vleck formula for testing hypothetical structural scenarios. This procedure is based on a two-spin SIMPSON calculation. To ensure that this approach is applicable to disordered inorganic systems such as glasses, we must examine the validity of this approach for multispin systems. Furthermore, an analysis of potential systematic errors arising from distributions of dipole$-$dipole coupling constants and nuclear electric quadrupolar interaction parameters is needed.

Multispin Effects. Although eq 5 is valid for two-spin interactions only, the second moment (M_2) analysis expressed by eq 8 should be actually independent of the order of the spin system. This is because the M_2 calculation implicitly approximates the multispin interaction by a summation of two-spin interactions (which is, of course, permissible only at sufficiently short dipolar evolution times). To ascertain that the approach of eq 8 can indeed be extended to multiple-spin systems, additional SIMPSON calculations were performed for SI_2 and SI_3 spin systems, respectively. Figure 7 illustrates the influence of the magnitude of C_q(^{23}Na) on the REDOR curves of a three-spin system ^{23}Na$-^{31}$P$-^{23}$Na, assuming an angle of

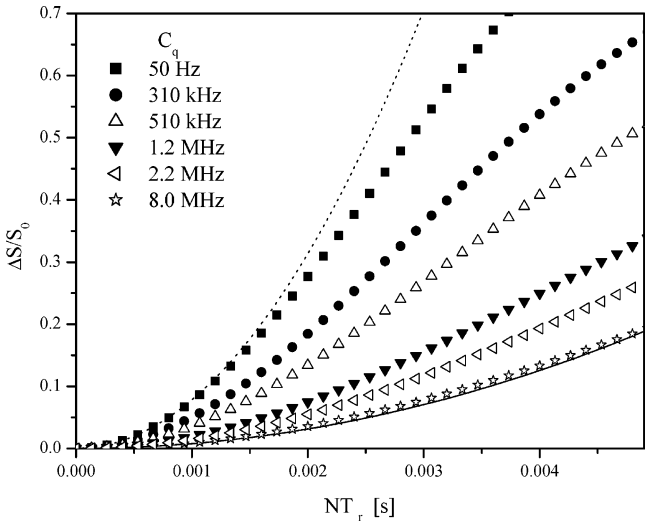

Figure 8. REDOR simulations for a four-spin system consisting of one P atom in the center of an equilateral triangle comprised of three Na atoms. The Na$-$P internuclear distances were chosen to be 0.57 nm. The SIMPSON simulations were performed assuming $\nu_1 = 55$ kHz and $\nu_r = 15$ kHz. C_q is systematically varied ($\eta = 0.5$). In addition, the nonselective case with $f_1 = 1$ (dotted line) and the selective case with $f_1 = 0$ (solid line) are sketched. The first situation ($f_1 = 1$) is identical to a parabolic fit of the nonselective case ($C_q = 50$ Hz) in the data range $\Delta S/S_0 < 0.2$, whereas the second situation ($f_1 = 0$) is identical to a fit of the selective case ($C_q = 8.0$ MHz) up to $\Delta S/S_0 < 0.2$.

TABLE 1: Calculated f_1 Values from eq 8 for the ^{23}Na$-^{31}$P$-^{23}$Na Three-Spin System for Different Values of the Dipolar Angle ζ

	f_1 value			
C_q	$\zeta = 0°$	$\zeta = 30°$	$\zeta = 60°$	$\zeta = 90°$
50 Hz	0.8843	0.9153	0.9345	0.9228
310 kHz	0.5370	0.5502	0.5687	0.5630
510 kHz	0.3334	0.3545	0.3638	0.3609
1.2 MHz	0.1174	0.1305	0.1395	0.1380
2.2 MHz	0.0559	0.0647	0.0704	0.0693
8.0 MHz	-0.0002	0.0043	0.0064	0.0052

$\zeta = 30°$ between the two dipolar vectors. Analogous simulations that have been performed for $\zeta = 0°$, 60°, and 90°, respectively, reveal that the influence of the spin geometry on the shape of the resulting REDOR curves is minimal at short dipolar evolution times. Table 1 summarizes the geometry dependence of the f_1 values for different C_q values, as obtained by fitting the corresponding REDOR curve to eq 8. Figure 8 summarizes the calculated dephasing for a single S-spin in the dipolar field of three quadrupolar I-spins, arranged in the form of an equilateral triangle. Again, the magnitude of ν_1/ν_q is the decisive parameter, producing the entire spectrum of REDOR behaviors from completely nonselective to fully selective excitation of the I-spin central transition. Overall, our simulations indicate that the variations of the M_2 values obtained by applying our procedure to arrangements with the same $\sum_I r_{IS}^{-6}$ values, but different specific geometries range within 10%, i.e., within the limits of experimental uncertainty. Furthermore, by restricting the analysis to the limit of short dipolar evolution times, the effect of homonuclear $I-I$ dipole interactions upon the $S\{I\}$ REDOR curve is minimized.[24]

Effect of Distributions of Dipolar Coupling Constants. A situation commonly encountered in disordered materials is that a distribution of internuclear distances exists, producing a continuous range of magnetic dipole$-$dipole coupling constants. This results in subtle changes in the REDOR curvature, affecting the quality of parabolic fits to expression 8. To explore the

systematic error encountered as a result of such distribution effects, composite REDOR curves were calculated for three different Gaussian distributions of internuclear distances, which translate to corresponding asymmetric distribution functions of dipolar coupling constants (see Figure 9), because $D \approx r^{-3}$. In these simulations, a fixed C_q value of 2.2 MHz was assumed, and a set of REDOR curves was calculated with SIMPSON, while incrementing the internuclear distance in steps of 0.005 nm, following a Gaussian profile. All of the resulting REDOR curves were then superimposed according to their respective weighting factors. In analogy to our previous simulation results for dipolar couplings between spin $-^1/_2$ systems only,[20] the oscillations observed for the isolated $S\{I = {}^3/_2\}$ spin-pair situation are quickly damped when a distribution of dipolar couplings is introduced (see Figure 9a). Furthermore, Figure 9b indicates that the distribution effects lead to a slightly increased curvature at short dipolar evolution times. As a result, a fit of experimental data to eq 8 will produce slightly enhanced M_2 values, as compared to the situation of a singular dipolar coupling constant. We predominantly believe that these increases in M_2 originate from the asymmetry of the distribution function of D, which occurs as the result of a symmetric distribution of r values. Still, within the limits of the widths of the distribution considered, we can conclude that the systematic error in M_2 arising from a distribution of dipolar coupling constants is of the same order of magnitude as the inherent experimental error of the analysis procedure (10%).

Effects of Distributions of Nuclear Electric Quadrupolar Coupling Constants. An even more serious concern about potential systematic errors arises from the well-known fact that nuclear electric quadrupolar coupling constants also are subject to distribution effects in disordered systems. Such distributions have two consequences: (i) the precision with which the pulse length chosen corresponds to a flip angle π and (ii) the extent to which outer Zeeman states contribute to S-signal dephasing are now variable from site to site. It is therefore evident that any such distribution function of C_q values translates to a corresponding distribution function of f_1 values, and the question arises in regard to which extent the average dipolar second moment value extracted from the experimental data via eq 8 will be affected by this. Generally, the impact of a C_q distribution on the REDOR curve is expected to be dependent on both the width and the central value considered. The decisive parameter is the slope df_1/dC_q, which, at any chosen value of the rf amplitude, obeys a specific dependence on C_q, as Figure 3 indicates. A special case arises for the limit of large quadrupolar splitting if the condition $\nu_1 \ll \nu_q$ holds across the entire distribution function of C_q. In this particular limiting situation (selective excitation of the central transition only), the REDOR curve should remain essentially unaffected by C_q distributions, provided that second-order quadrupolar line broadening effects do not interfere with a uniform excitation across the NMR powder pattern. As revealed by Figure 3a and 3b, these predictions are indeed confirmed by the simulation results. Figure 10 shows the effect of C_q distributions for quadrupolar splittings that are of intermediate and moderately large magnitudes. Three exemplary cases are presented for central C_q values of 0.7 MHz (distribution function increment of 0.1 MHz) and 2.2 MHz (distribution function increment of 0.2 MHz), respectively, where, in the latter case, two different widths of the Gaussian distributions have been considered. A rotor frequency of 15 kHz and an rf amplitude corresponding to $\nu_1 = 55$ kHz have been assumed in these simulations, the latter implying 180° pulse lengths of 6.8 and 5.6 μs, respectively, for those ^{23}Na spins

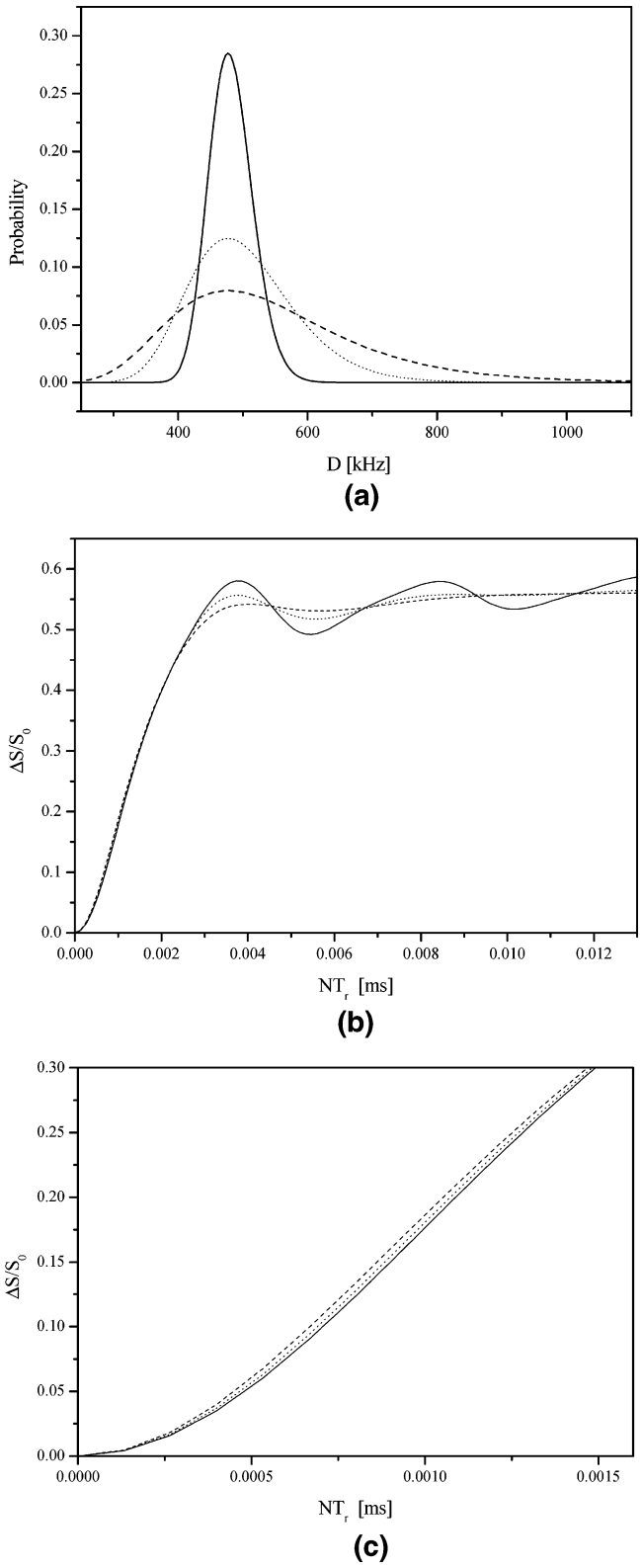

Figure 9. Simulated ^{31}P{^{23}Na} REDOR results, according to distributions of dipolar couplings; a C_q value of 2.2 MHz ($\eta = 0.5$) was assumed. Panel a shows the distributions of dipolar coupling constants resulting from Gaussian distance distributions ((—) $\sigma = 0.07$ Å, (···) $\sigma = 0.16$ Å, and (- - -) $\sigma = 0.25$ Å). Panel b shows the resulting REDOR curves; the distribution with $\sigma = 0.07$ Å leads to a curve that is indistinguishable from the simple two-spin case. Panel c shows the initial regime curvature that produces the enhanced M_2 values of 103% and 108%, relative to the value with no distribution, for (···) $\sigma = 0.16$ Å and (- - -) $\sigma = 0.25$ Å, respectively.

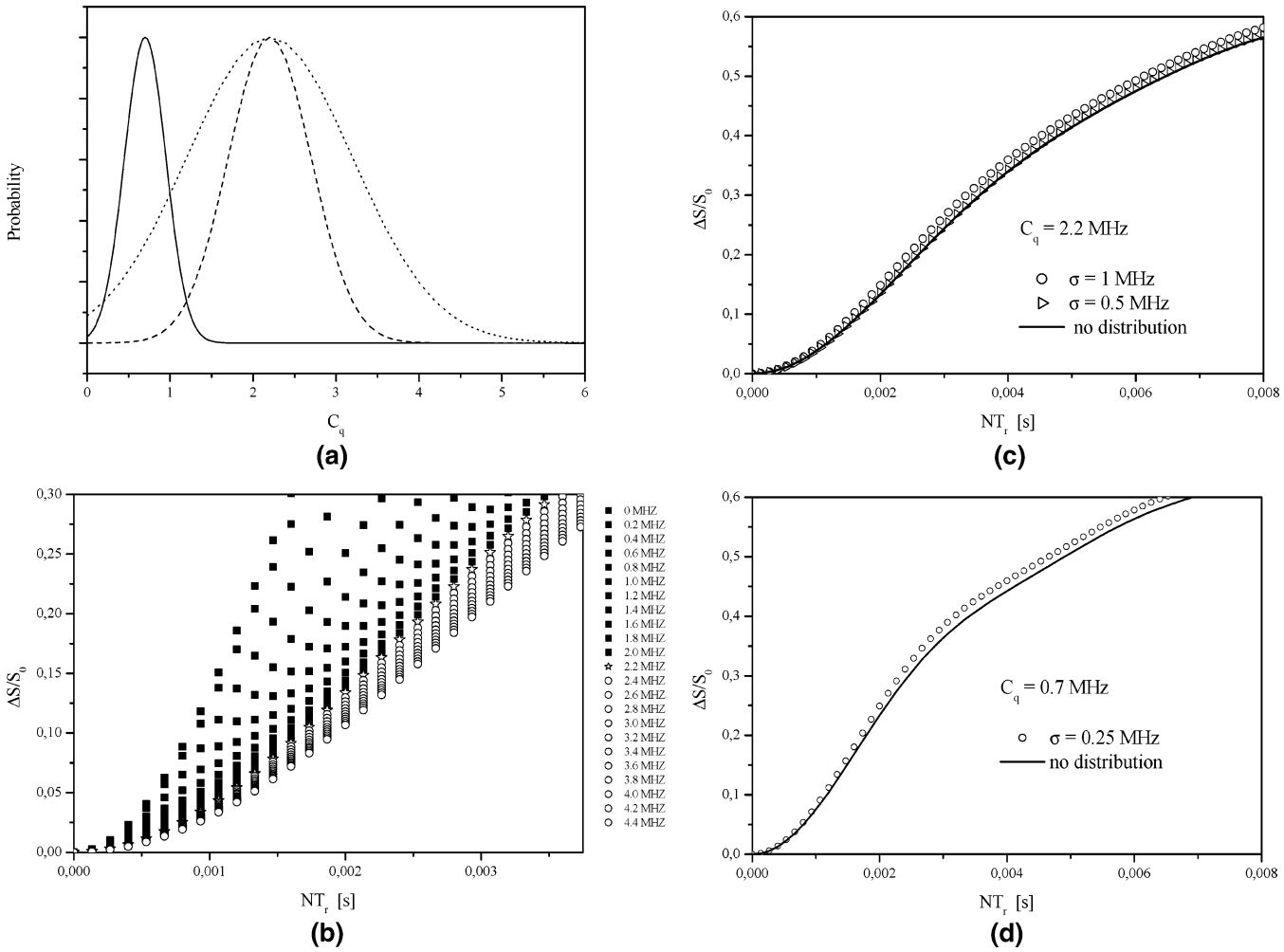

Figure 10. Effect of Gaussian distributions of quadrupolar coupling constants on the REDOR curves: (a) three distributions, with central values of (—) $C_q = 0.7$ MHz ($\eta = 0.5$) and $\sigma = 0.25$ MHz, (- - -) $C_q = 2.2$ MHz ($\eta = 0.5$) and $\sigma = 0.5$ MHz, and (···) $C_q = 2.2$ MHz ($\eta = 0.5$) and $\sigma = 1$ MHz; (b) example of REDOR curves with $C_q = 2.2$ MHz, $\eta = 0.5$, and $\sigma = 1$ MHz; (c) resulting Gaussian-weighted superposition of REDOR curves according to Figure 10b with $C_q = 2.2$ MHz, where the resulting M_2 values, in terms of the percentage of the ideal value ($\sigma = 0$), are 102% ($\sigma = 0.5$ MHz) and 114% ($\sigma = 1$ MHz); and (d) superposition with $C_q = 0.7$ MHz and $\sigma = 0.25$ MHz, where the resulting M_2 value is 110%, compared to the value with no distribution.

TABLE 2: Summary of the NMR Parameters of the Crystalline Sodium Phosphates

			Averaged Value				M_2 ($\times 10^6$ s^{-2})[a]	
C_q (MHz)	η	relative intensity (%)	C_q (MHz)	η	ν_1/ν_q[b]	f_1, from eq 8	van Vleck	measured
				$Na_3P_3O_9$				
1.57	0.55	66.6	1.81	0.55	0.0746	0.0980	26.5	27.9 (105%)
2.30	0.71	33.3						
				$Na_4P_2O_7$				
2.08	0.26	25	2.63	0.50	0.0604	0.0700	52.9	57.5 (109%)
2.90	0.47	25						
2.30	0.70	25						
3.22	0.56	25						
				Na_3PO_4				
3.15	0.30	33.3	2.64	0.49	0.0412	0.0505	78.8	74.0 (94%)
2.20	0.93	33.3						
1.92	0.47	16.7						
3.55	0	8.3						
2.85	0	8.3						

[a] Values in parentheses indicate the percentage of the van Vleck value, which was calculated from the crystal structure. The duty cycles in all measurements are 4%−8%, depending on the spinning speed. (No deviations between the data measured at two spinning speeds could be detected, because of the small difference in the duty cycle.) [b] The slight differences in the ν_1/ν_q values result from minor variations in the experimental conditions (^{23}Na π-pulse lengths).

having the above-stated C_q values. Although all three of these conditions produce a widely spread multitude of highly divergent REDOR/REAPDOR curves for different spin pairs for each of these cases, the superposition of these manifolds (the actual observable) deviates only slightly from the curves calculated on the basis of uniform average C_q values. Ignoring the distribution thus results in slight overestimations (~10%) of the dipolar M_2 values only. Thus, our simulations suggest that the

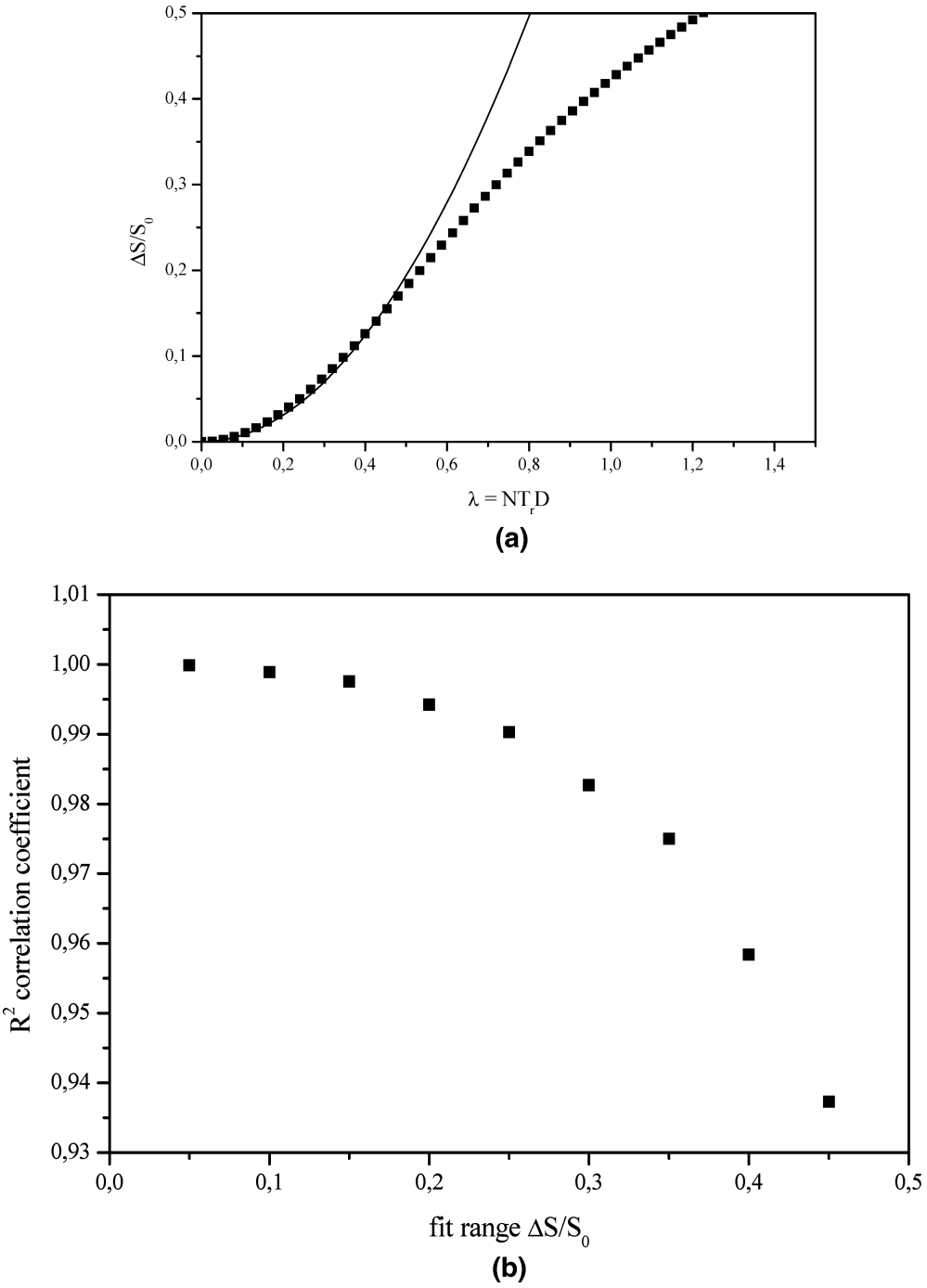

Figure 11. (a) Example of a calculated REDOR curve (squares), adopting experimental parameters and parabolic fit (solid curve) in the data range $\Delta S/S_0 < 0.2$. (b) Dependence of the quality (squared correlation coefficient, R^2) of the parabolic fit on the $\Delta S/S_0$ data range; the dramatic decrease in fit quality justifies the limitation of the data range to $0 < \Delta S/S_0 < 0.2$, as described in the text.

initial curvature analysis reflected by eq 8 is a fairly robust method, producing average dipolar coupling information that is essentially unaffected by distribution effects of nuclear electric quadrupolar coupling constants.

Experimental Validation on Model Compounds. To validate the approach delineated previously, we report and analyze $^{31}P\{^{23}Na\}$ REDOR data for the crystalline model compounds $Na_3P_3O_9$, $Na_4P_2O_7$, and Na_3PO_4. Table 2 summarizes the nuclear electric quadrupolar coupling parameters extracted from ^{23}Na MQMAS NMR and available from the literature. Based on this information, the universal $^{31}P\{^{23}Na\}$ REDOR curves were calculated numerically. All three model compounds present Na ions on multiple sites; therefore, weighted averages of the C_q values were used in these calculations. For each of the calculated curves, the early decay region $0 < \Delta S/S_0 < 0.2$ was fitted to a parabola (eq 8, Figure 11), producing the efficiency factors f_1 listed in Table 2. As revealed by Figure 11b, the quality of the parabolic fit diminishes dramatically if the data range is increased beyond $\Delta S/S_0 = 0.2$. Therefore, it is essential to limit this analysis to the early decay region.

Figure 12 shows experimental REDOR data for the three model compounds considered, along with parabolic fits to eq 8, where the above-determined f_1 values have been used. Because of the dependence of f_1 on the applied nutation frequency ν_1 and the duty cycle (Figure 5), care was taken to conduct the simulations under exactly the same conditions (ν_1 value, MAS rotor speed) that were used for recording the experimental data. As indicated in Table 2, the experimental

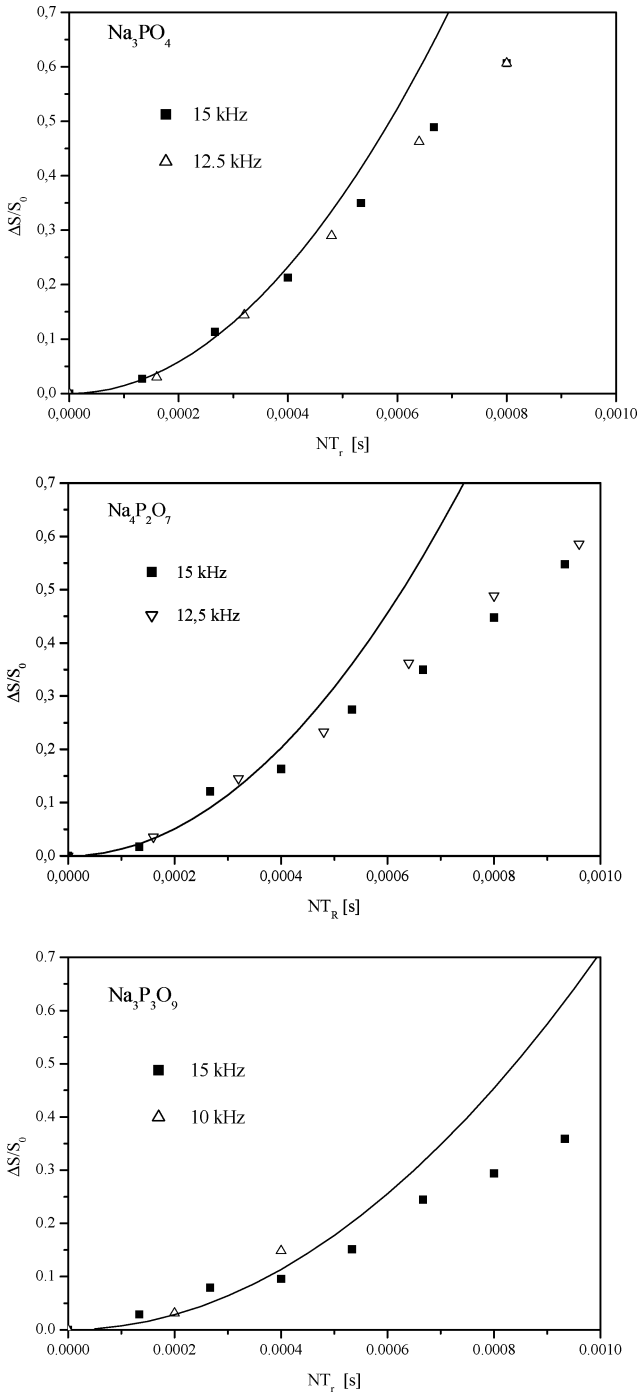

Figure 12. Experimental REDOR data for the crystalline model compounds $Na_3P_3O_9$, $Na_4P_2O_7$, and Na_3PO_4. Solid lines are parabolic fits to the data regime $\Delta S/S_0 < 0.2$. Each REDOR curve was measured at two different MAS spinning speeds, to increase the number of data points in the initial regime.

M_2 values determined in this manner are in good agreement with the theoretically expected values calculated from the internuclear distances, using the van Vleck equation. Thus, we can conclude that the moments method introduced here is reasonably robust to produce reliable dipolar coupling information.

Application to Phosphate Glasses. Figure 13 shows experimental REDOR curves for two binary sodium phosphate glasses, containing 60% and 35% sodium oxide, respectively. Since the $Q^{(3)}$, $Q^{(2)}$, and $Q^{(1)}$ sites are well-resolved by MAS NMR,[37] site-selective dipolar coupling information is available for the two different types of phosphate units. The corresponding information is collected in Table 3. This analysis is based on a SIMPSON simulation, using the experimental C_q values and an arbitrarily chosen η value. In view of the η dependence of f_1, noted in Figure 3b, only a range of M_2 values can be specified, because the asymmetry parameter in the glasses is not known and likely is subject to some distribution. Table 3 also includes a "best-guess" value (given in parentheses) extracted from the experimental REDOR curve by assuming a uniform η distribution in the glass.

Overall, the range of possible values is sufficiently narrow to permit a chemical interpretation of the experimental results. Clearly, the magnitude of the ^{23}Na dipolar field present at the ^{31}P site increases as the number of nonbridging O atoms increases. This behavior is similar to that observed qualitatively[8] in previous studies of silicate glasses. Because the overall local charge requiring cationic compensation increases from zero to two along the sequence $Q^{(3)} \rightarrow Q^{(2)} \rightarrow Q^{(1)}$, the observed experimental effect is not unexpected. For both the $Q^{(2)}$ and $Q^{(1)}$ sites, the corresponding M_2 values measured in the glasses are similar to those obtained for the prototype crystalline model compounds. Still, the M_2 values measured for the $Q^{(2)}$ sites in the glasses also increase significantly as the sodium content in the glass increases. This finding reflects the proximity of $Q^{(1)}$ and $Q^{(2)}$ sites in the network, leading to the establishment of Na−O−Na proximities in the glass at higher sodium contents. Finally, the neutral $Q^{(3)}$ site also displays dipolar coupling of significant strength to ^{23}Na nuclei, although no charge compensation is needed for this site. This finding suggests that the nonbridging O atoms of these $Q^{(3)}$ sites participate in the Na coordination to some extent. All of these results are consistent with a statistical alkali-ion distribution in the glass, rather than cation clustering or even phase separation. Our conclusions are nicely consistent with previous conclusions drawn from $^{31}P\{^{23}Na\}$ variable-contact-time cross-polarization experiments[38] and also with those from recent $^{31}P\{^{7}Li\}$ REDOR results of lithium phosphate glasses.[39]

Discussion and Conclusions

In summary, we have developed a robust rotational echo double resonance (REDOR) procedure to extract reliable site-resolved dipolar coupling information in unspecified multispin systems containing quadrupolar nuclei. By restricting the analysis to a determination of initial curvature, we can extract distinct second moment (M_2) information for all of those peaks that are resolved in the magic angle spinning (MAS) NMR spectrum of the observed nuclei, and this information is not influenced by the specifics of the distance geometry (i.e., the number of spins interacting, the orientations of the relevant distance vectors involved, and the relative orientations of dipolar and electric field gradient (EFG) tensors). The method does require a priori information about the nuclear electric quadrupolar coupling constants of the *I*-nuclei, which is easily available from appropriate single-pulse or multiple quantum MAS experiments. Because radio-frequency (rf) irradiation during MAS induces adiabatic transitions between the various Zeeman levels of the quadrupolar *I*-nuclei, the REDOR response is strongly influenced by the experimental conditions (rotor frequency ν_r, rf amplitude ν_1, and duty cycle). The latter effects are accounted for, however, by comparing the experimental REDOR data with SIMPSON simulations based on the same conditions that were applied experimentally. Finally, the approach can be applied to multispin interactions as well, and distribution effects of nuclear dipole−dipole and/or nuclear electric quadrupolar coupling interactions introduce only minor systematic errors. All of these

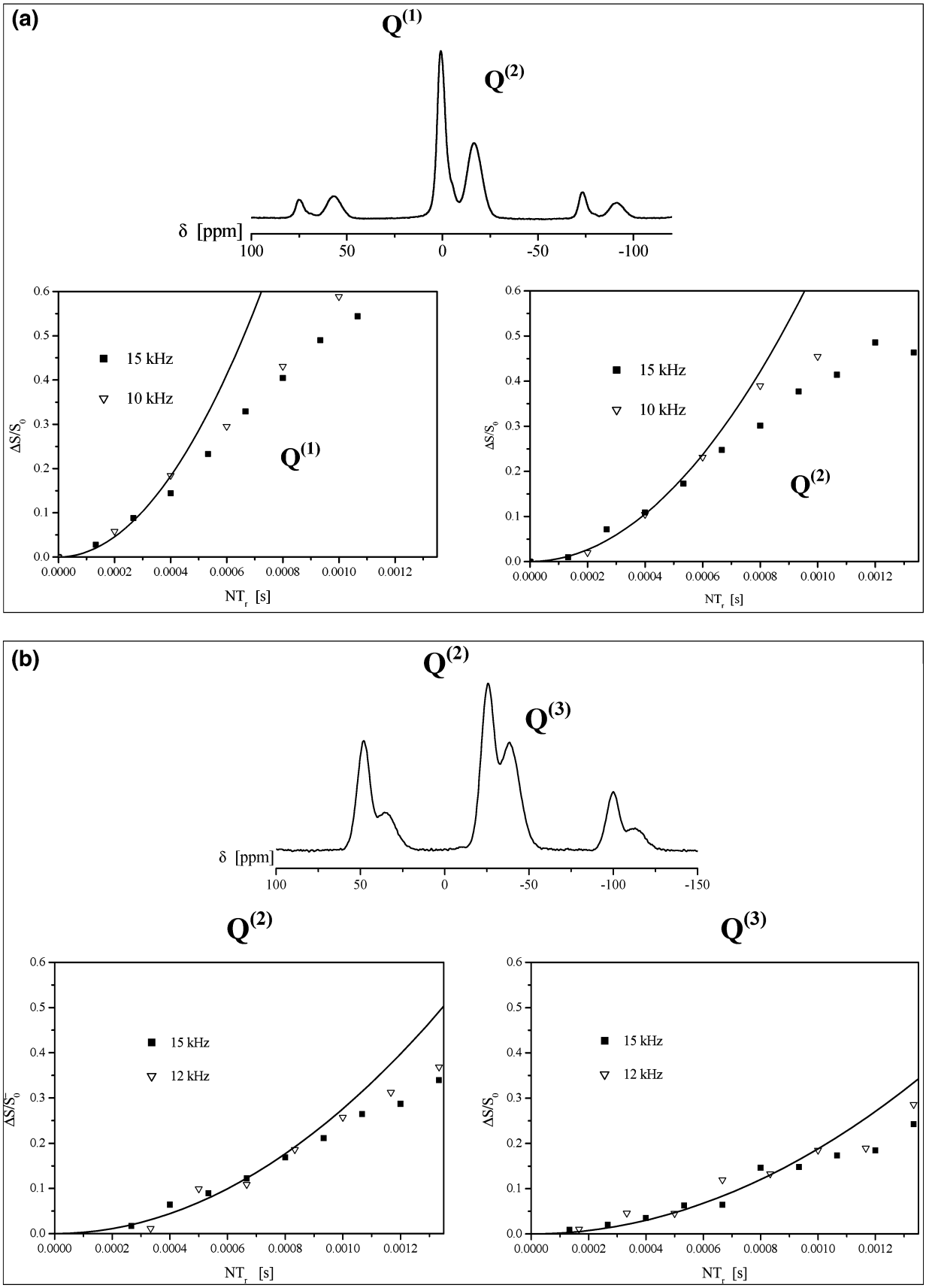

Figure 13. Summary of the experimental results on two sodium phosphate glasses with composition (a) $0.6Na_2O{\cdot}0.4P_2O_5$ and (b) $0.35Na_2O{\cdot}0.65P_2O_5$. Each ^{31}P spectrum shows two distinguishable peaks, corresponding to different $Q^{(n)}$ units. By fitting the ^{31}P echo and dephasing spectra, including the spinning sidebands, REDOR curves for each $Q^{(n)}$ unit are obtained. These were analyzed on the basis of f_1 values obtained by assuming the experimental C_q value and $\eta = 0.5$ in the analysis via eq 8. The resulting second moments (M_2 values) are summarized in Table 3.

TABLE 3: Experimental Results for the Two Glass Compositions[a]

η	f_1	M_2 ($\times 10^6$ s^{-2})[b]
60% Na_2O−40% P_2O_5, SOQE = 2.03 MHz, $\nu_1/\nu_q = 0.0666$		
0	0.0675	$Q^{(1)}$ 52.7 ± 2.1
0.5	0.0776	49.9 ± 1.9
1	0.101	44.3 ± 1.6 (49.0 ± 1.8)
0	0.0675	$Q^{(2)}$ 30.3 ± 1.1
0.5	0.0776	28.7 ± 1.0
1	0.101	25.5 ± 0.9 (28.2 ± 1.0)
35% Na_2O−65% P_2O_5, SOQE = 1.98 MHz, $\nu_1/\nu_q = 0.0470$		
0	0.0478	$Q^{(2)}$ 14.3 ± 0.5
0.5	0.0540	13.8 ± 0.5
1	0.0740	12.3 ± 0.4 (13.5 ± 0.5)
0	0.0478	$Q^{(3)}$ 8.9 ± 0.3
0.5	0.0540	8.6 ± 0.3
1	0.0740	7.6 ± 0.3 (8.4 ± 0.3)

[a] Depending on the η-value assumed, slightly different f_1 values are extracted, translating to a range of M_2 values. The second-order quadrupolar effect (SOQE) is defined as SOQE = $C_Q\sqrt{1 + (^1/_3\eta^2)}$ and was also determined using the MQMAS method, which yields, in this case, only an average value of SOQE. [b] Values in parentheses assume a uniform η distribution in the analysis.

features make this procedure uniquely well-suited for the structural analysis of disordered inorganic systems and glasses. The work of the present study has shown that the accuracy of the M_2 measurement is generally ~10% for crystalline compounds, whereas for glasses, the cumulative error that results from the effects of unknown geometries and wide dipolar and quadrupolar coupling distributions may result in larger errors.

In our view, the main advantage of our approach over the transfer of populations with double resonance (TRAPDOR) and rotation echo adiabatic passage double resonance (REAPDOR) methods lies in the fact that, because of the short irradiation times, the spin dynamics of the quadrupolar *I*-spins are kept as simple as possible. Generally, it seems advisable to conduct all the experiments and simulations at duty cycles below 10%, to mimimize adiabatic spin-state transfers. Furthermore, if varying spinning frequencies are applied in the experiment to generate more data points for the initial curvature analysis, an inspection of the experimental data must be done to ensure that the f_1 changes caused by the concomitant duty-cycle variations are indeed tolerable. We can expect the latter not to be a major problem if the experimental conditions chosen correspond to very small ν_1/ν_q values.

It is appropriate here to discuss our method in relation to other existing approaches in the literature, which may be promising for the structural analysis of glasses in the future. The method presented here is complementary to the recent technique published by Amoureux et al.,[40] who have extended the frequency-selective REDOR approach[41] to SI_n multiple-spin systems where the observed species *S* represents the quadrupolar nucleus, whereas $I = {}^1/_2$. For the case of observed spin $-{}^1/_2$ systems coupled to quadrupolar nuclei, two rather simple procedures have been published recently for the case of two-spin systems, which do not require knowledge of the strength of the nuclear electric quadrupolar coupling parameters. Saalwächter and Schmidt-Rohr have exploited the *S*-spin dephasing resulting from longitudinal relaxation of directly coupled quadrupolar *I*-spins for distance measurements in $S\{I = 1\}$ spin pairs (relaxation-induced dipolar exchange with recoupling, RIDER),[42] and Gullion and co-workers have presented a simple analysis procedure of REAPDOR data for the $S\{I = 1\}$and $S\{I = {}^5/_2\}$ two-spin cases.[43−45] In the latter work, it was shown that, within a certain experimental regime defined by specific boundaries of ν_1/ν_q and ν_1/ν_r, REAPDOR data may actually be analyzed in terms of a universal analytical formula in the absence of any knowledge regarding the nuclear electric quadrupolar interactions. Using this approach, the authors were able to measure $^{13}C-{}^2H$ internuclear distances from REAPDOR data. For future studies, it will be of great interest to explore whether this method, as well as RIDER, might be transferable to the $S\{I = {}^3/_2\}$ case, and whether they can be extended to include many-spin interactions. Although both of these alternative approaches are very attractive, because of their simplicity, their applicability may be less general and limited by specific boundary conditions concerning spin−lattice relaxation times and experimental conditions imposed by the ν_1/ν_q and ν_1/ν_r ratios. Therefore, we consider it worthwhile also to extend our approach to other systems including $I = {}^5/_2$ nuclei, as well as to spin interactions involving two different types of quadrupolar nuclei.

Acknowledgment. Funding by the Sonderforschungsbereich SFB 458 is most gratefully acknowledged. W.S. thanks the Fonds der Chemischen Industrie for a doctoral stipend.

References and Notes

(1) Eckert, H. *NMR* **1994**, *33*, 125.
(2) Ernst, R. R.; Bodenhausen, G.; Wokaun, A. *Principles of Nuclear Magnetic Resonance in One and Two Dimensions*; Clarendon Press: Oxford, U.K., 1987.
(3) Schmidt-Rohr, K.; Spiess, H. W. *Multidimensional Solid-State NMR and Polymers*; Academic Press: London, 1996.
(4) Gullion, T.; Schaefer, J. *J. Magn. Reson.* **1989**, *81*, 196.
(5) Gullion, T. *Magn. Reson. Rev.* **1997**, *17*, 83.
(6) Gullion, T. *Concepts Magn. Reson.* **1998**, *10*, 277.
(7) Gullion, T.; Schaefer, J. *J. Magn. Reson.* **1991**, *92*, 439.
(8) van Wüllen, L.; Gee, B.; Züchner, L.; Bertmer, M.; Eckert, H. *Ber. Bunsen−Ges. Phys. Chem.* **1996**, *100*, 1539.
(9) Fyfe, C. A.; Mueller, K. T.; Grondey, H.; Wong-Moon, K. C. *J. Phys. Chem.* **1993**, *97*, 13484.
(10) Fyfe, C. A.; Lewis, A. R. *J. Phys. Chem. B* **2000**, *104*, 48.
(11) Schaller, T.; Rong, C.; Toplis, M. J.; Cho, H. J. *J. Non-Cryst. Solids* **1999**, *248*, 19.
(12) Holl, S.; Schaefer, J. *Solid State Nucl. Magn. Reson.* **1996**, *6*, 39.
(13) Prabakar, S.; Wenslow, R. M.; Mueller, K. T. *J. Non-Cryst. Solids* **2000**, *263&264*, 82.
(14) Janssen, M.; Eckert, H. *Solid State Ionics* **2000**, *136−137*, 1007.
(15) Egan, J. M.; Wenslow, R. M.; Mueller, K. T. *J. Non-Cryst. Solids* **2000**, *261*, 115.
(16) Chan, J. C. C.; Bertmer, M.; Eckert, H. *J. Am. Chem. Soc.* **1999**, *121*, 5238.
(17) Vogt, F. G.; Gibson, J. M.; Mattingly, S. M.; Mueller, K. T. *J. Phys. Chem. B* **2003**, *107*, 1272.
(18) Fyfe, C. A.; Brouwer, D. H.; Lewis, A. R. *J. Am. Chem. Soc.* **2002**, *124*, 7770.
(19) Naito, A.; Nishimura, K.; Tuzi, S. *Chem. Phys. Lett.* **1994**, *229*, 506.
(20) Bertmer, M.; Eckert, H. *Solid State Nucl. Magn. Reson.* **1999**, *15*, 139.
(21) Chan, J. C. C.; Eckert, H. *J. Magn. Reson.* **2000**, *140*, 170.
(22) Bertmer, M.; Züchner, L.; Chan, J. C. C.; Eckert, H. *J. Phys. Chem. B* **2000**, *104*, 6541.
(23) van Vleck, J. H. *Phys. Rev.* **1948**, *74*, 1168.
(24) Goetz, J. M.; Schaefer, J. *J. Magn. Reson.* **1997**, *127*, 147.
(25) van Eck, E. R. H.; Janssen, R.; Maas, W. E. J. R.; Veeman, W. S. *Chem. Phys. Lett.* **1990**, *174*, 428.
(26) Grey, C. P.; Vega, A. J. *J. Am. Chem. Soc.* **1995**, *117*, 8232.
(27) Gullion, T. *Chem. Phys. Lett.* **1995**, *246*, 325.
(28) Gullion, T. *J. Magn. Reson., Ser. A* **1995**, *117*, 326.
(29) Chopin, L.; Vega, S.; Gullion, T. *J. Am. Chem. Soc.* **1998**, *120*, 4406.
(30) Kalwei, M.; Koller, H. *Solid State Nucl. Magn. Reson.* **2002**, *21*, 145.
(31) Garbow, J. R.; Gullion, T. *J. Magn. Reson.* **1991**, *95*, 442.
(32) Mueller, K. T. *J. Magn. Reson., Ser. A* **1995**, *113*, 81.
(33) Schmidt, A.; Mackay; R. A.; Schaefer, J. *J. Magn. Reson.* **1992**, *96*, 644.
(34) Hudalla, C.; Eckert, H.; Dupree, R. *J. Phys. Chem.* **1996**, *100*, 15986.

(35) Bak, M.; Rasmussen, J. T.; Nielsen, N. C. *J. Magn. Reson*. **2000**, *147*, 296.
(36) Ba, Y.; Kao, H. M.; Grey, C. P.; Chopin, L.; Gullion, T. *J. Magn. Reson*. **1998**, *133*, 104.
(37) Brow, R. K.; Kirkpatrick, R. J.; Turner, G. L. *J. Non-Cryst. Solids* **1990**, *116*, 39.
(38) Prabakar, S.; Wenslow, R. M.; Mueller, K. T. *J. Non-Cryst. Solids* **2000**, *263&264*, 82.
(39) van Wuellen, L.; Schwering, G.; Eckert, H. *Chem. Mater*. **2000**, *12*, 1840.
(40) Trebosc, J.; Amoureux, J. P.; Wiench, J. W.; Pruski, M. *Chem. Phys. Lett.* **2003**, *374*, 432.
(41) Jaroniec, C. P.; Tounge, B.; Herzfeld, J.; Griffin, R. G. *J. Am. Chem. Soc*. **2001**, *123*, 3507.
(42) Saalwächter, K.; Schmidt-Rohr, K. *J. Magn. Reson*. **2000**, *145*, 161.
(43) Gullion, T. *J. Magn. Reson*. **2000**, *146*, 220.
(44) Hughes, E.; Gullion, T.; Goldbourt, A.; Vega, S. Vega, A. J. *J. Magn. Reson*. **2002**, *156*, 230.
(45) Goldbourt, A.; Vega, S.; Gullion, T.; Vega, A. J. *J. Am. Chem. Soc*. **2003**, *125*, 11194.